Morphological Studies on Extruded Films and Filaments of Polypropylene

R. JANARTHANAN, S. N. GARG, and A. MISRA*

Centre for Materials Science & Technology, Indian Institute of Technology, New Delhi-110016, India

SYNOPSIS

In the present work, an attempt has been made to study the development of morphology during extrusion and uniaxial stretching of polypropylene (PP) films and filaments at corresponding conditions. Dies for extrusion of films and filaments were designed to achieve similar extrusion velocity and shear rates. Orientation in films and fibers of PP produced from these dies was determined by birefringence and wide-angle X-ray diffraction (WAXD). The degree of crystallinity was determined by density and WAXD. The superstructure developed during extrusion was studied in films by small-angle light scattering. It was inferred that films and fibers prepared under similar conditions would produce similar morphology. Hence, films can be characterized by optical techniques when it is difficult to study fibers. © 1994 John Wiley & Sons, Inc.

INTRODUCTION

The main purpose of this work was to prepare films and fibers under identical conditions. The principle proposed by Han[1,2] was used for this, which suggests that similar flow properties are attained when films and/or fibers are extruded at equivalent shear rates and comparable extrusion velocities. The fibers can easily be characterized by techniques such as birefringence and wide-angle X-ray diffraction (WAXD). However, they cannot easily be characterized for the superstructures by techniques such as optical microscopy or small-angle light scattering (SALS). On the other hand, films can be studied by light microscopy and SALS. In this study, SALS was employed to characterize extruded PP films. The equivalence in properties of films and fibers was evaluated.

EXPERIMENTAL

Fabrication of Dies and Sample Preparation

The dies for extrusion of films and filaments were designed to achieve similar processing conditions in both the cases. Extrusion velocity, shear rates, and take-up velocity were matched for the extrusion of films and filaments assuming that the fluid behaved like a power law fluid in the shear rate range of interest.[1-4] Figure 1 shows a plot of log shear stress vs. log shear rate, which is a straight line with a power law exponent (n) of 0.4.

For a capillary die, the shear rate ($\dot{\gamma}$) for a non-Newtonian fluid is given by

$$\dot{\gamma}_{cap} = 2V(n + 3)/D$$

where $\dot{\gamma}_{cap}$ is the shear rate in a capillary die used to make fiber samples; n, the power law exponent; V, the extrusion velocity; and D, the diameter of the capillary.

The flow in a rectangular die can be considered similar to the flow between two parallel infinite plates if the width of the die is much greater than the thickness "t." In such a case, the shear rate for a non-Newtonian flow can be given as

$$\dot{\gamma}_{rec} = 2V(n + 2)/t$$

where $\dot{\gamma}_{rec}$ is the shear rate in a rectangular die used to make films and t is the thickness.

Equating the shear rates for both dies,

$$2V(n + 3)/D = 2V(n + 2)/t$$

* To whom correspondence should be addressed.

Journal of Applied Polymer Science, Vol. 51, 1175–1182 (1994)
 CCC 0021-8995/94/071175-08

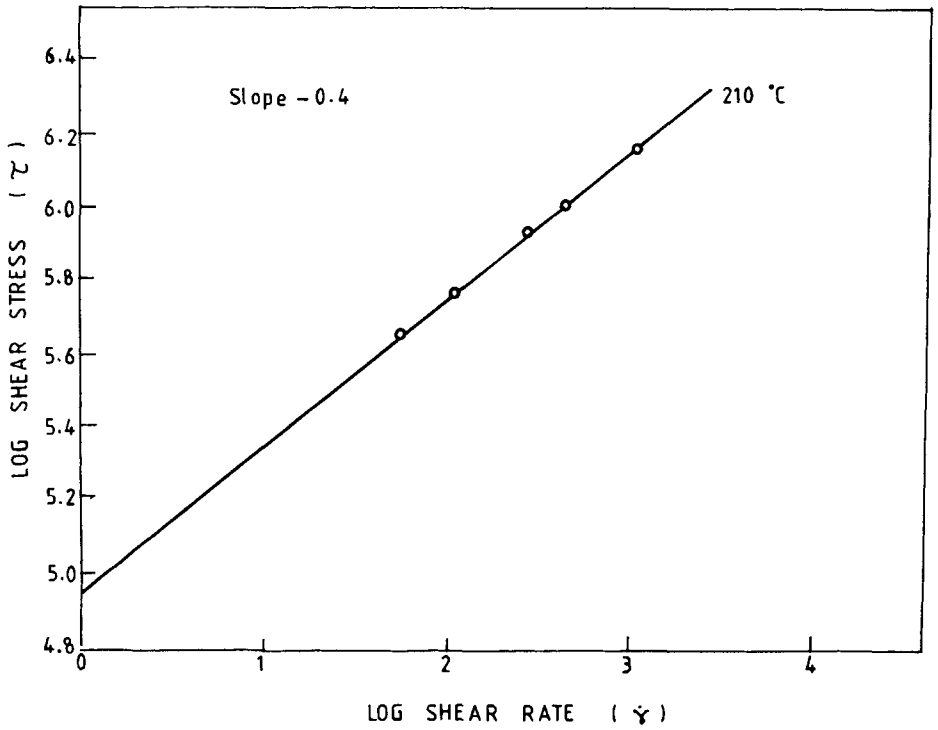

Figure 1 Plot of shear stress as a function of shear rate for PP.

Keeping the extrusion velocity the same, we get

$$D/t = (n + 3)/(n + 2)$$

This expression gives the ratio of diameter of a fiber die to the slit thickness in order to achieve the same shear rates assuming the velocities in both the dies are identical. In the present case, the capillary diameter was selected to be 0.07 cm. Thus, the thickness of the slit die can be calculated as

$$t = D(n + 2)/(n + 3) = 0.05 \text{ cm}$$

Width of the slit die was taken to be 25 times the thickness. The die width then would be 1.25 cm.

In the above geometries, the output rate of the film would be much larger than that from the fiber die. On the other hand, the velocity in the fiber die could not be reduced due to the limitations of the extruder. Thus, a five-filament die with five holes was made to overcome these difficulties. Matching extrusion velocities were determined for these dies by extruding the polymer at various extrusion rates. Final take-up velocities were selected to give jet-stretch ratios of 5, 10, 15, 20, 25, and 30, respectively. However, the actual jet-stretch values were calculated from the denier and the area of cross section of the resulting stretched fiber and film.

Sample Preparation

Isotactic polypropylene (PP) with the trade name GWM22, obtained from Indian Petrochemicals Co., was used for these studies. The melt viscosity of the polymer was measured using an Instron capillary at 210°C and at shear rates of 70–1000 s^{-1}. The polymer was found to be non-Newtonian with a power law exponent of 0.4. A $\frac{3}{4}$ in. single-screw extruder from Betol Machinery, England, was employed for extruding films and fibers.

CHARACTERIZATION

Birefringence of each sample was measured using a compensator attached to a polarizing microscope. An average of 10 specimens was taken for each measurement. Density measurements were made at 25°C using a Davenport density gradient column from which weight fraction crystallinity values were calculated. The density values of amorphous and crystalline PP were taken as 0.852 and 0.937 gm/cm, respectively.[5]

WAXD measurements were conducted to calculate the crystallinity, crystallite size, and crystalline orientation function. For crystallinity, the powdered sample was compressed in a rectangular orifice that

was then mounted on the rotating stage of Phillips X-ray unit and scanned with a diffractometer from 5 to 40°. Miller's approach[6] was employed to calculate the crystallinity index as isotactic PP cannot be prepared in amorphous form. X-ray diffraction patterns were obtained at 30 kV and 20 mA with an exposure time of 4 h. Wilchinsky's generalized method[7] was utilized to calculate the orientation function, since no pure (001) plane is available in the unit cell structure of isotactic PP. The crystal orientation function was calculated using Herman's approach. The amorphous orientation function was calculated, assuming the validity of a two-phase model for the polymer, by Stein's method.[8] The crystallite size was calculated from Scherrer's formula using the (040) plane.

Stress–strain behavior of these samples was observed on a Universal Instron testing machine. Twenty-five specimens were tested for each sample. SALS was used to determine the size of superstructure that formed in the films. The methods proposed by Samuels[9] and Pakula[10] were used to estimate the size of the deformed spherulites.

RESULTS AND DISCUSSION

Figure 2 is a plot of birefringence as a function of jet stretch for films and filaments. There is a clear observation that the birefringence value increases with an increase in jet stretch irrespective of the shape of the sample. The increase along the same slope suggests similar orientational development at corresponding states. According to the theory of spinning orientation, the orientation development is governed by streaming orientation within the spinneret channel, which, in turn, depends on extrusion velocity.[11] The orientation along the spinning path is developed by two mechanisms, namely, streaming orientation in the elongational flow and deformation orientation. In a free fluid subjected to an axial tension, the force controlling the orientation is the parallel velocity gradient that would depend on the difference between the take-up velocity (V_L) and extrusion velocity (V_e). Deformational orientation may either be irreversible (plastic) or reversible (elastic). In both cases, the orientation factor is determined by the factor in (V_L/V_e). However, deformational orientation is considered as the limiting case of non-steady-state streaming orientation with a zero diffusion rate. Earlier studies on spinning have revealed strong effects on the velocity difference ($V_L - V_e$) rather than on the ratio of the two (V_L/V_e). In materials like PP, where the relaxation times are large, the effects of ($V_L - V_e$) have been observed, suggesting some contribution from the deformational orientation. In the present case, it is suggested that the streaming orientation in the spinneret, streaming orientation in the elongational flow, and the deformational orientation are equal in

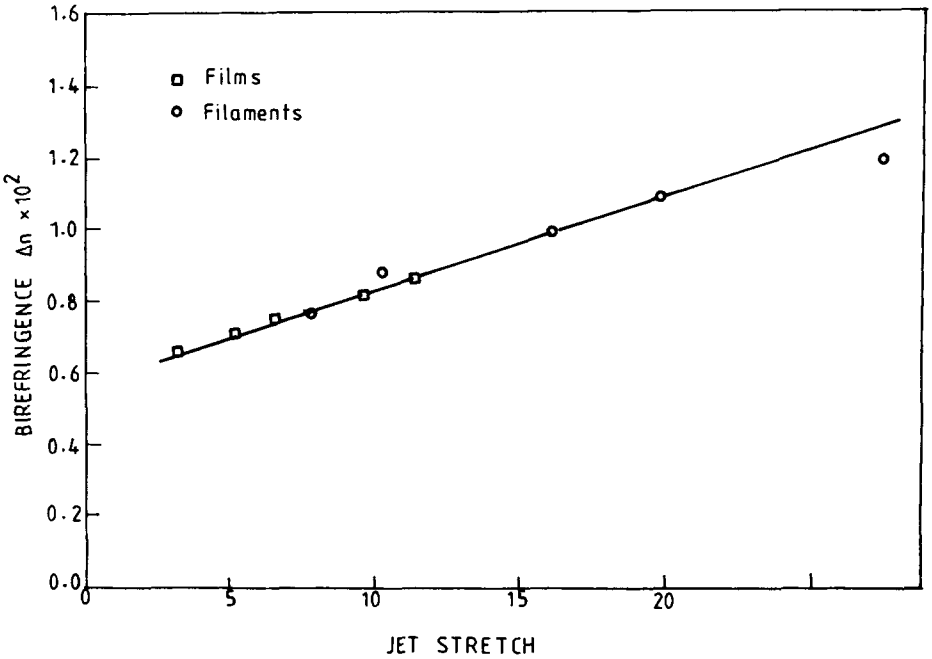

Figure 2 Plot of birefringence as a function of jet stretch for PP.

both cases and therefore similar overall orientation levels are observed in both films and fibers.

Crystallinity of the samples in the as-spun state was calculated using density as well as the X-ray technique. It was surprising to note that all the samples had about the same density level of 0.916 g/cm, which corresponds to a crystallinity of about 77%. WAXD data also provided similar results, and crystallinity in all samples was at the level of about 72%. The crystallinity development in melt-spun fibers is controlled mainly by the rate of crystallization, time available for cooling, molecular orientation, heat-transfer coefficient, and temperature of the cooling medium. Earlier studies have shown that the increase in spinning rate increases molecular orientation, which, in turn, decreases the half-time of crystallization.[12] At higher take-up speeds, the residence time of the melt decreases at a time when crystallization is at a maximum. Since crystallinity is a function of both, the increase in one and decrease in another probably led to similar crystallinity values.

Figure 3 shows a plot of Herman's orientation function (f_c) and amorphous orientation function (f_a) as a function of actual jet stretch. It can be seen that f_c increases with increase in the jet stretch. This would be expected because of the higher mechanical force present at higher jet-stretch ratios. The values are low because the samples are in an as-spun or as-extruded state. Moreover, the final take-up velocities are also relatively low. The major effect of the hydrodynamics of the extrusion process in the present case appears to be that of partial chain alignment, which facilitates nucleation. The crystal orientation is similar at corresponding jet-stretch ratios irrespective of the configurational differences. Amorphous orientation function values also follow a similar trend as observed in the case of crystal orientation and have not been influenced by the film/filament configurational difference. Figure 4 shows a plot of crystallite size as a function of the jet-stretch ratio. The decrease in the crystal size with increasing jet stretch may be due to the breakup of lamellae at high jet-stretch values.

Figure 5 shows a plot of tensile strength and strain at break as a function of jet-stretch ratio. The tensile strength increased while the strain at break decreased with increase in the jet-stretch ratio. This

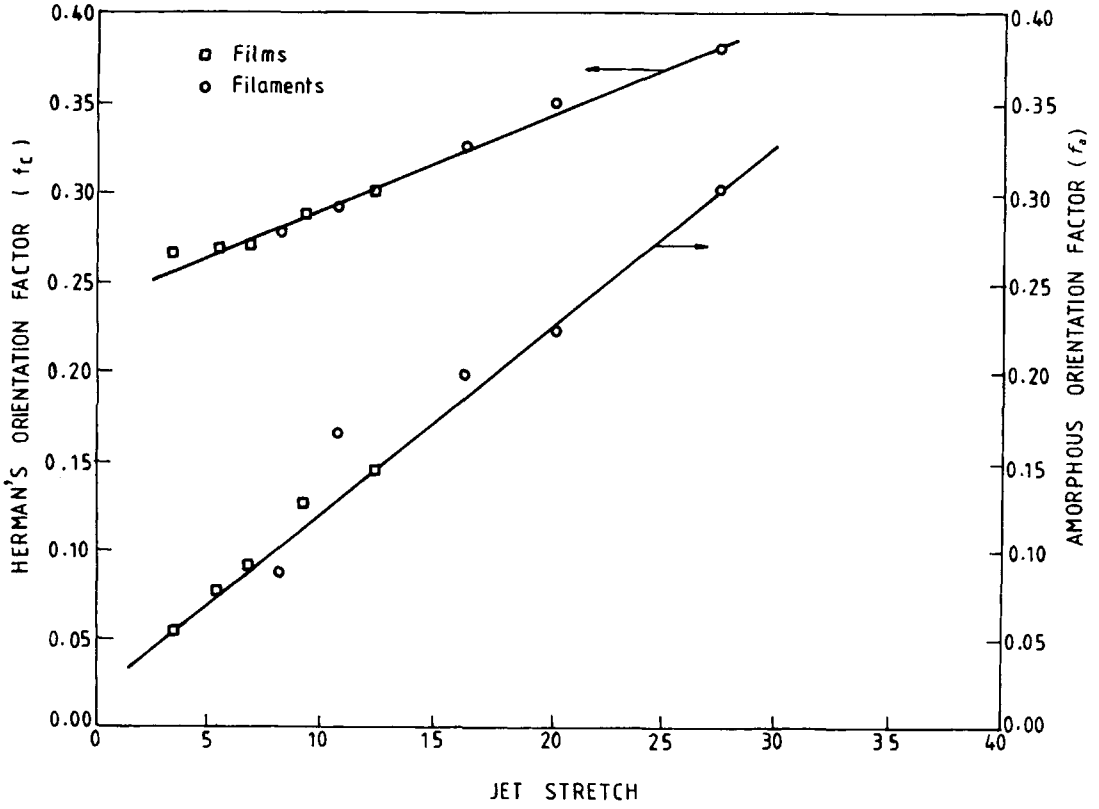

Figure 3 Plot of Herman's orientation function (f_c) and amorphous orientation function (f_a) vs. jet stretch for PP.

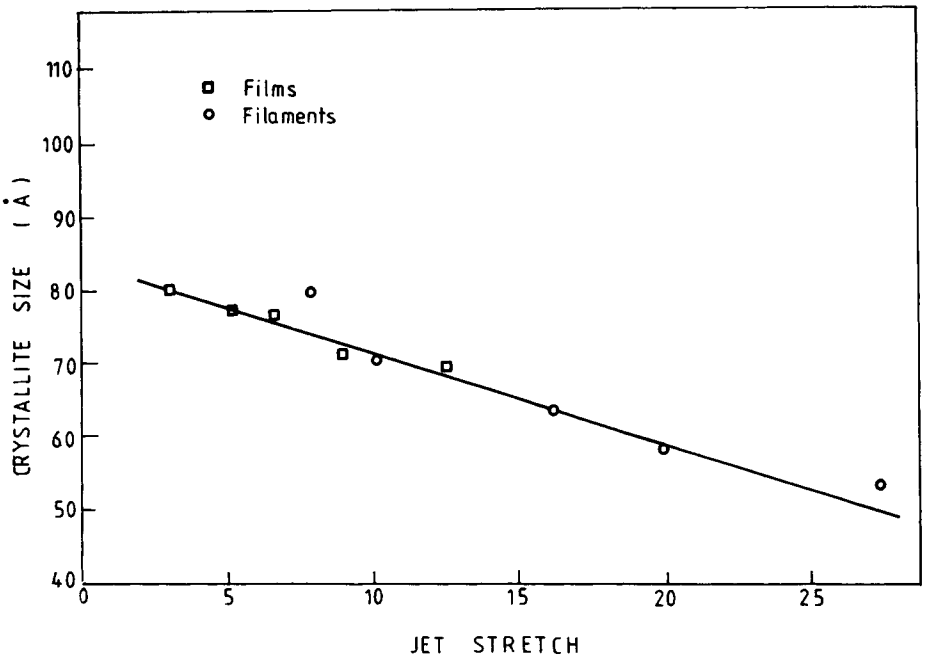

Figure 4 Plot of crystallite size as a function of jet stretch for PP.

can be attributed to decrease in crystal size and increase in the orientation of crystals with increase in the jet-stretch values.

SALS experiments were carried out to study the development of the superstructure. Figure 6 shows H_v light-scattering patterns for films with different jet-stretch values that are typical of those obtained from PP.[8-10] The four lobe patterns, which are preferentially oriented toward one of the polars, are typical of the patterns observed from deformed spher-

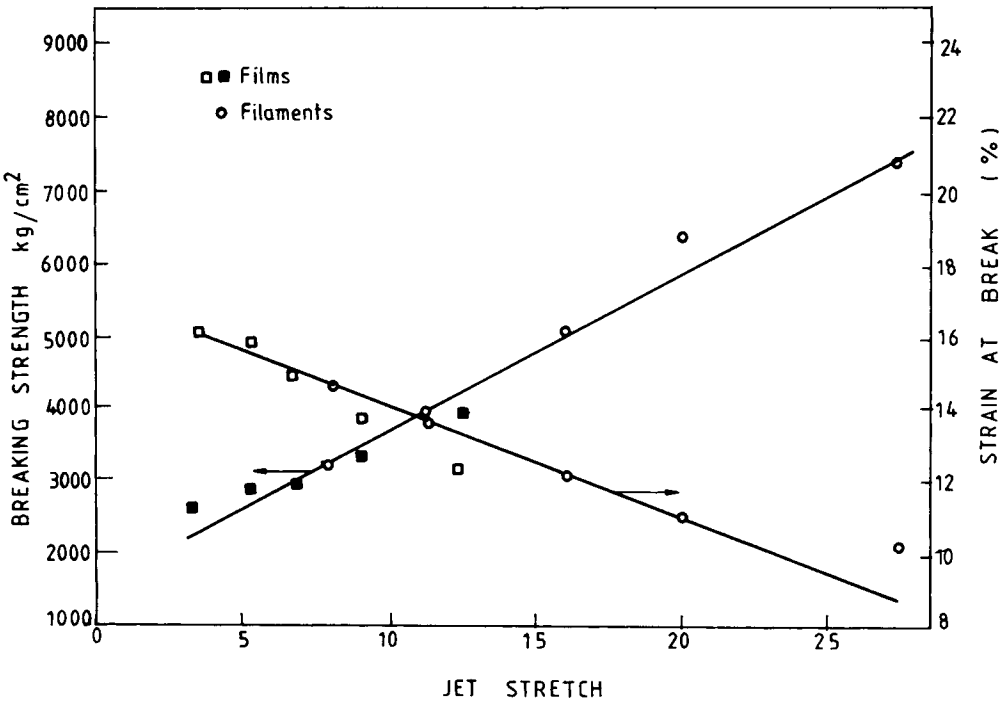

Figure 5 Plot of tensile strength and strain at break as a function of jet stretch for PP.

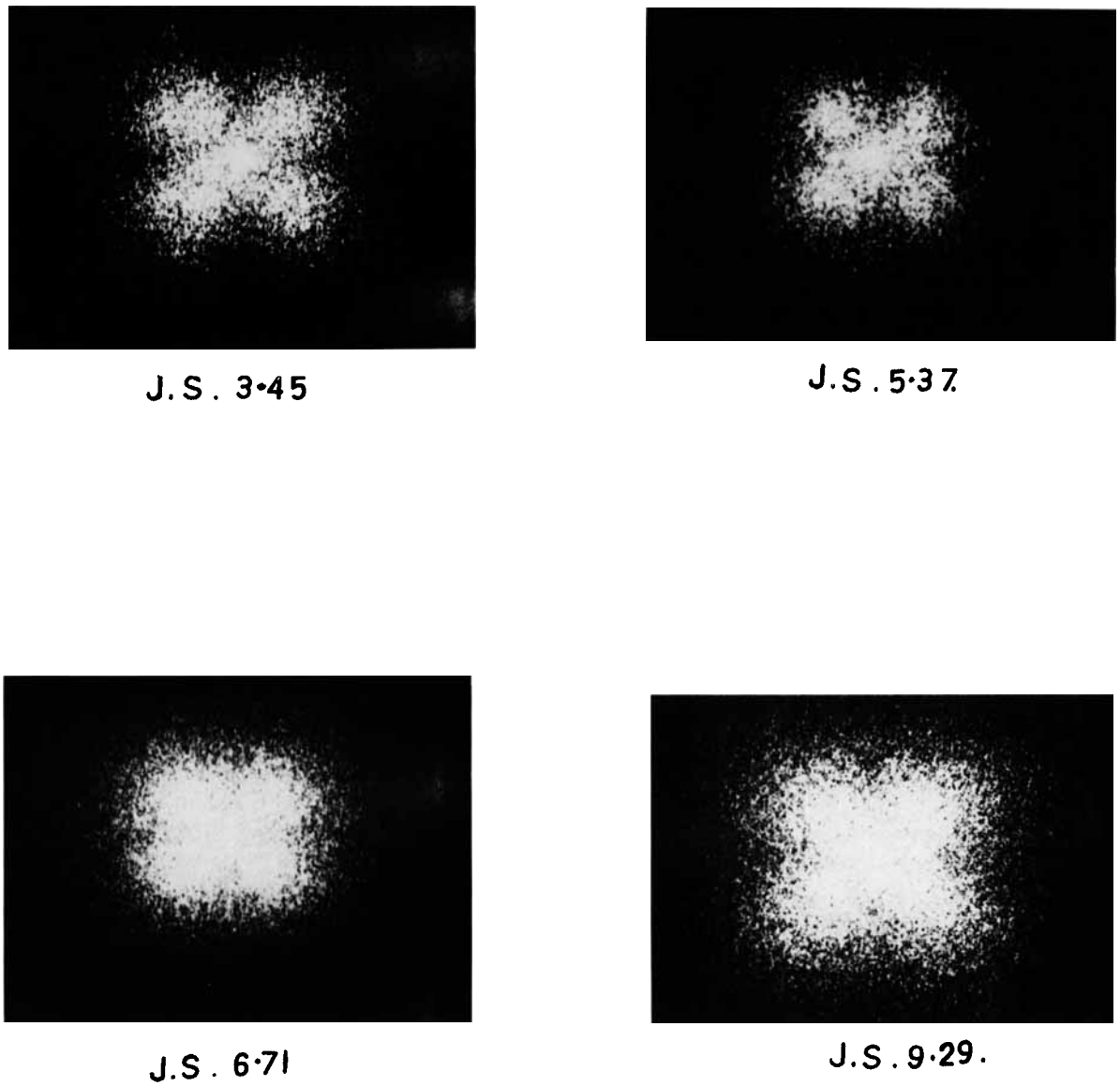

Figure 6 Series of SALS patterns in extruded films as a function of jet stretch for PP.

ulites.[8-10] Similar patterns have been observed by Gasparyan and Baranov[13] for melt-oriented samples of polycaprolactam. The tilt in the scattering lobes increased as the jet-stretch ratio increased. In the case of melt-oriented systems, the molecules are already in a partially oriented state before nucleation. Once the polymer begins to solidify, the spherulite formation starts, the fibrillar growth across the jet stretch is preferred, and, hence, the spherulite growth in the transverse direction is enhanced. Figure 7 shows a plot of the elongational ratio of spherulites as a function of the jet-stretch ratio using Samuels'[9] and Pakula's[10] models. The size of spherulites, as if it was in the undeformed state, is plotted in Figure 8. The spherulite size decreased as the jet-stretch ratio increased. The decrease in size levels off beyond jet-stretch ratio of about six.

CONCLUSIONS

It is clear from the above studies that filaments and films extruded at corresponding conditions have similar properties that give support to the approach that it is possible to use results for one to predict those in the other. Orientation studies for structural characterization can be easily carried out on extruded thin films by optical techniques. The results

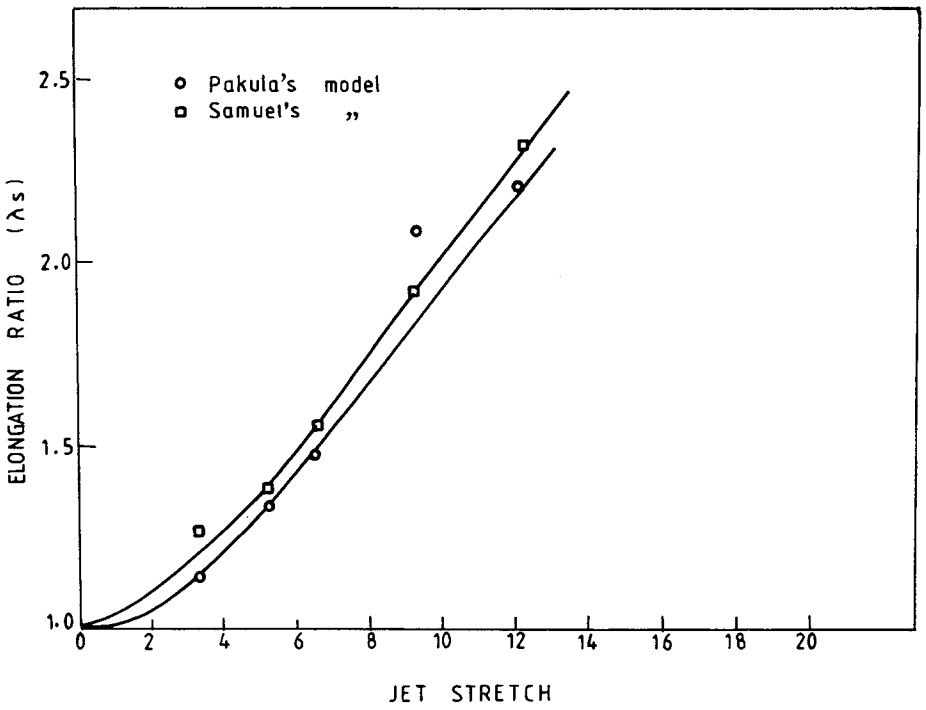

Figure 7 Plot of elongational ratio of spherulites in extruded films as a function of jet stretch for PP.

can be applied for predicting the formation of structure in fibers made under identical conditions. Such an analysis has considerable potential for an indirect analysis of the superstructure developed in fibers since optical techniques such as SALS cannot be easily applied for fibers.

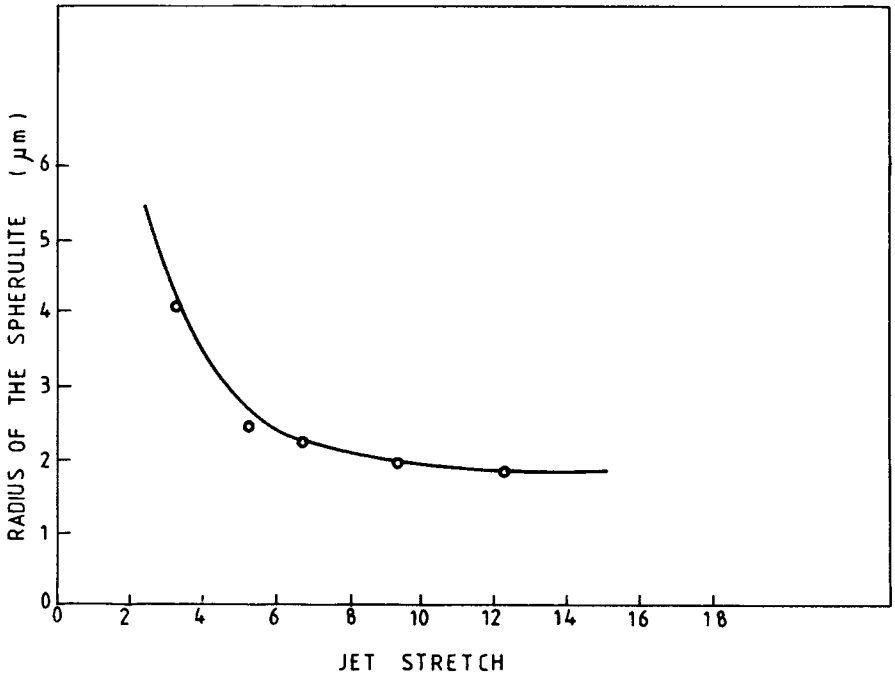

Figure 8 Plot of size of spherulites in extruded films as a function of jet stretch for PP.

REFERENCES

1. C. D. Han, *J. Appl. Polym. Sci.*, **15,** 1149 (1971).
2. C. D. Han, *J. Appl. Polym. Sci.*, **15,** 2567 (1971).
3. S. Middleman, *Fundamentals of Polymer Processing,* McGraw Hill, New York, 1970.
4. C. D. Han, *Rheology in Polymer Processing,* Academic Press, New York, 1970.
5. J. Brandrup and E. H. Immergut, *Polymer Handbook,* Wiley, New York, 1975.
6. R. L. Miller, in *Encyclopedia of Polymer Science and Technology,* N. M. Bikales, Ed., Wiley Interscience, New York, 1969, Vol. 4, p. 449.
7. J. W. Wilchinsky, *J. Appl. Phys.*, **31,** 1969 (1960).
8. R. S. Stein, in *Structure & Properties of Polymer Films,* R. W. Lenz and R. S. Stein, Eds., Gordon and Breach, New York, 1977.
9. R. J. Samuels, *J. Polym. Sci. A2,* **9,** 2165 (1971).
10. T. Pakula and M. Kryzeweski, *J. Polym. Sci. C,* **38,** 87 (1979).
11. Z. K. Walczak, *Formation of Synthetic Fibers,* Gordon and Breach, New York, 1977.
12. R. J. Samuels, *Structured Polymer Properties,* Wiley, New York, 1974.
13. K. A. Gasparyan and V. G. Baranov, *J. Polym. Sci. A2,* **8,** 1015 (1975).

Received January 12, 1993
Accepted July 23, 1993